Deficiency of alkaline SMase enhances dextran sulfate sodium-induced colitis in mice with upregulation of autotaxin[1]

Ping Zhang,[2,*] Ying Chen,[†,§] Tao Zhang,[*] Jiang Zhu,[*] Lei Zhao,[*] Jianshuang Li,[*] Guangzhi Wang,[*] Yongchun Li,[*] Shuchang Xu,[†] Åke Nilsson,[§] and Rui-Dong Duan[2,§]

Medical Laboratory Science and Technology College,* Harbin Medical University, Daqing Campus, Daqing, China; Department of Gastroenterology,† Tongji Institute of Digestive Diseases, Tongji Hospital, Tongji University School of Medicine, Shanghai, China; and Gastroenterology and Nutrition Laboratory,§ Department of Clinical Sciences, Lund University, Lund, Sweden

Abstract **Intestinal alkaline SMase (Alk-SMase) cleaves phosphocholine from SM, platelet-activating factor (PAF), and lysophosphatidylcholine. We recently found that colitis-associated colon cancer was 4- to 5-fold enhanced in Alk-SMase KO mice. Here, we further studied the pathogenesis of colitis induced by dextran sulfate sodium (DSS) in WT and KO mice. Compared with WT mice, KO mice demonstrated greater body weight loss, more severe bloody diarrhea, broader inflammatory cell infiltration, and more serious epithelial injury. Higher levels of PAF and lower levels of interleukin (IL)10 were identified in KO mice 2 days after DSS treatment. A greater and progressive increase of lysophosphatidic acid (LPA) was identified. The change was associated with increased autotaxin expression in both small intestine and colon, which was identified by immunohistochemistry study, Western blot, and sandwich ELISA. The upregulation of autotaxin coincided with an early increase of PAF. IL6 and TNFα were increased in both WT and KO mice. At the later stage (day 8), significant decreases in IL6, IL10, and PAF were identified, and the decreases were greater in KO mice. In conclusion, deficiency of Alk-SMase enhances DSS-induced colitis by mechanisms related to increased autotaxin expression and LPA formation. The early increase of PAF might be a trigger for such reactions.**—Zhang, P., Y. Chen, T. Zhang, J. Zhu, L. Zhao, J. Li, G. Wang, Y. Li, S. Xu, Å. Nilsson, and R-D. Duan. **Deficiency of alkaline SMase enhances dextran sulfate sodium-induced colitis in mice with upregulation of autotaxin.** ***J. Lipid Res.*** **2018.** 59: **1841–1850.**

Supplementary key words lysophosphatidic acid • nucleotide pyrophosphatase phosphodiesterase 2 • nucleotide pyrophosphatase phosphodiesterase 7 • platelet activating factor • interleukin 10 • interleukin 6 • tumor necrosis factor α • sphingomyelinase

Alkaline SMase (Alk-SMase) was originally identified as an enzyme that hydrolyzes SM to ceramide in the intestinal tract (1). Studies with Alk-SMase KO mice have confirmed the crucial role of the enzyme in SM digestion (2). Alk-SMase is an ecto-enzyme that anchors on the mucosal membrane with a short hydrophobic domain, and is released into the lumen in an active form by bile salt and pancreatic trypsin (3). The enzyme shares no structural similarities with acid and neutral SMases, but belongs to the ecto-nucleotide pyrophosphatase phosphodiesterase (NPP) family (4). As a novel member of the family, Alk-SMase is also called NPP7.

Further characterizations of purified and recombinant Alk-SMase revealed that it is a phosphocholine-specific enzyme that cleaves the phosphocholine group not only from SM but also from platelet-activating factor (PAF) (5) and lysophosphatidylcholine (lyso-PC) (4). These effects render the enzyme important implications in carcinogenesis and inflammation, because the metabolism of these substrates is deeply involved in inflammation and cancer (6–8). In line with this hypothesis, dietary SM was previously found to inhibit carcinogen-induced colon cancer in animals (9) and progressive reduction of Alk-SMase activity was found in patients with ulcerative colitis, sporadic adenomas, colonic carcinomas, and familial adenomatous polyposis (10–13). Recently, we found that colitis-associated

This work was supported by National Natural Science Foundation of China Grant 81500407, 57th General Financial Postdoctoral Science Foundation Grant 2015M571435, Heilongjiang Postdoctoral Science Foundation Grant LBH-Z15144 in China, and grants from Cancerfonden, the Albert Påhlsson Foundation, the Crafoord Foundation, and the Region Skåne University Hospital Foundation in Sweden.

Manuscript received 10 February 2018 and in revised form 4 August 2018.

Published, JLR Papers in Press, August 7, 2018
DOI https://doi.org/10.1194/jlr.M084285

This article is available online at http://www.jlr.org

Abbreviations: Alk-SMase, alkaline sphingomyelinase; DAI, disease activity index; DSS, dextran sulfate sodium; IBD, inflammatory bowel disease; IHC, immunohistochemistry; IL, interleukin; LPA, lysophosphatidic acid; LPD, lysophospholipase D; lyso-PC, lysophosphatidylcholine; NPP, nucleotide pyrophosphatase phosphodiesterase; PAF, platelet-activating factor.

[1] A portion of the results of this paper was selected for a poster presentation at the American Association for Cancer Research (AACR) annual meeting, Shanghai, China, November 5–8, 2016.

[2] To whom correspondence should be addressed.
e-mail: pingxin2003@163.com (P.Z.); Rui-dong.duan@med.lu.se (R-D.D)

colon cancer was enhanced in Alk-SMase KO mice (14), indicating that the anticancer properties of Alk-SMase are linked to its anti-inflammatory effects.

Considering the three major substrates of Alk-SMase, its anti-inflammatory effect may be more closely related to its activity against PAF and lyso-PC, which are two pro-inflammatory phospholipids (7, 15). Increased PAF has been found in inflammatory diseases in the intestine and liver (16, 17). By cleaving phosphocholine from PAF, Alk-SMase inactivates PAF and blocks PAF-induced MAP kinase activation, chemotaxis, and cytokine release (5); and by cleaving phosphocholine from lyso-PC, Alk-SMase converts lyso-PC to monoacylglycerol, which may decrease formation of lysophosphatidic acid (LPA) by lysophospholipase D (LPD) (3). LPA has emerged as a potent inflammatory factor that activates multiple signal transduction pathways, such as Ras, Rac, and PI3 kinase, to promote inflammation via different receptors (18). LPA is mainly generated by an enzyme called autotaxin, which was first identified as a nucleotidase and then turned out to be an important LPD for LPA generation (19, 20). Similar to Alk-SMase, autotaxin is a member of the NPP family, and is named NPP2 (21). The aim of this study was to examine the changes of colitis induced by dextran sulfate sodium (DSS) in WT and Alk-SMase KO mice, with particular attention paid to the changes of PAF, LPA, and autotaxin. Our study demonstrated that deficiency of Alk-SMase (NPP7) enhanced colitis with upregulation of autotaxin (NPP2) and increased formation of LPA and PAF.

MATERIALS AND METHODS

Animals

The Alk-SMase KO mice were generated as reported previously (2). The genetic background of the mice was C57BL/6. Deletion by Cre recombinase induces a shift of reading frame, which creates an early stop codon, resulting in blocking the translation of the transcript at early stage. Both WT and Alk-SMase KO mice used in this study were bred from intercross of heterozygous mice and then further bred to get enough animals for the investigation. The genotype and phenotype of the animals were confirmed by PCR and fecal Alk-SMase assay, as reported before. All mice were housed in the animal facilities at Daqing campus, Harbin Medical University and fed commercial standard pellets with free access to water. The mice were euthanized by cervical dislocation under inhaled isoflurane anesthesia. The experimental protocols were approved by the Animal Ethics Committee of Harbin Medical University, China.

Materials

DSS with a molecular mass of 36–50 kDa was purchased from MP Biomedicals (Stockholm, Sweden). The kits for analysis of PAF, LPA, interleukin (IL)10, IL6, and TNFα were purchased from Cloud-Clone Corp., USA (Wuhan, China). The antibody against autotaxin was purchased from Abcam (Shanghai, China) and the goat against mouse IgG antibody conjugated with horseradish peroxidase was from MXB Biotechnologies, China. The sandwich ELISA kit for autotaxin quantification was purchased from Echelon Biosciences Inc. (Salt Lake City, UT). The kit for mouse occult blood assay was purchased from ACON Biotechnologies Company (Hangzhou, China).

Induction of colitis by DSS and score of disease activity index

The colitis was induced by DSS treatment as previously described (22). At 9 weeks of age, both WT and KO mice were provided with 3% DSS dissolved in sterilized drinking water ad libitum for 8 days. The body weight was measured every day at 9:00 AM and the changes in percentage related to the original body weight on day 0 were calculated. The properties of the stools and the blood stain around the anus were examined. When no visible blood stain was found on the stools, the occult blood tests were performed. The disease activity index (DAI) was scored based on the weight loss, stool consistency, and blood in stool as shown in **Table 1**, which is essentially according to Maines et al. (23).

Examination of gross changes of tissues

The mice were euthanized on day 8 after DSS treatment. The colon was removed and its length measured from the ileocecal valve to the end of rectum. The segments were cut open and the gross changes of the tissue, including degrees of edema, bleeding, and ulceration, were examined under a dissecting microscope and scored according to **Table 2** (23). The liver, spleen, and thymus were removed and their wet weights determined.

Histopathology characterization

A proximal part (1 cm) of colon was cut and fixed in 4% paraformaldehyde, embedded in paraffin, further cut in 0.5 mm sections, and stained with H&E. The ulcerations, infiltration of inflammatory cells, crypt loss, epithelial cell hyperplasia, goblet cell reduction, and epithelial regeneration were examined in 10 randomly selected fields under microscopy and scored according to **Table 3** (23). For statistical analysis, the histology scores from each observed field were summed up and multiplied with the percentage of the fields with positive findings.

Determinations of PAF, LPA, IL6, IL10, and TNFα by ELISA

To determine the changes of PAF, LPA, and cytokines, both WT and KO mice were treated with DSS and euthanized on days 0, 2, 4, and 8, respectively. The colon was removed, cut open longitudinally, and rinsed with saline solution. The colonic mucosa was scraped and homogenized in lysis buffer containing 50 mM Tris, 150 mM NaCl, 1% Triton X-100, 1% sodium deoxycholate, 1% SDS, and 1 mM PMSF. After centrifugation, the supernatant was collected and the levels of IL6, IL10, TNFα, PAF, and LPA were determined by individual ELISA kits following the manufacturer's instructions.

Immunohistochemistry study on expression of autotaxin

The animals were treated with DSS as above and euthanized on days 0, 2, 4, and 8. A 0.5 cm-long segment was taken from the middle of the small intestine and colon of both WT and KO mice and fixed in 4% paraformaldehyde overnight and embedded in paraffin. The section was deparaffinized, followed by boiling in sodium citrate buffer (pH 6) for 20 min for antigen retrieval. The section was incubated with anti-NPP2 antibody for 15 min and then with goat against mouse IgG antibody conjugated with horseradish peroxidase for 30 min at room temperature. Diaminobenzidine (MXB Biotechnologies, China) was used as the chromogen. The section was then counterstained with hematoxylin and observed under a microscope.

Western blotting for autotaxin

To semi-quantify the autotaxin expression in the WT and KO mice, Western blot was performed 4 days after DSS treatment; as at this time point, expression of autotaxin was clearly demonstrated in immunohistochemistry (IHC) studies in both small

TABLE 1. Assessment of DAI

Score	Weight Loss	Stool Consistency	Blood in Stool
0	None	Normal pellets	Negative
1	1–5%	Slightly loose but in shape	Hemoccult positive
2	5–10%	Loose pellet	Visual slightly bleeding
3	10–15%	Loose feces and no shape	Obvious bleeding but no adhesion around anus
4	>15%	Diarrhea	Gross bleeding and blood incrustation around anus

intestine and colon, and LPA levels were significantly increased. The mucosal tissues from both small intestine and colon were scraped, homogenized, and centrifuged. Proteins of 50 μg of the supernatant were separated by 10% SDS-PAGE and transferred to a nitrocellulose membrane electrophoretically. After blocking with fat-free milk, the membrane was incubated with anti-NPP2 antibody (1:400) for 2 h, and then with goat anti-mouse IgG antibody conjugated with horseradish peroxidase (ZSGB-Bio, Beijing, China) for 1 h. The bands were identified by ECL advance reagents and the remitted light was recorded on X-ray film. The densities of the bands were measured by Image J software (National Institutes of Health; https://imagej.nih.gov/ij/).

Determination of autotaxin by sandwich ELISA

To confirm the Western blot results, a quantitative sandwich ELISA was employed to measure autotaxin levels in the homogenates of the small intestine and colon after DSS treatment for 4 days. According to the instructions of the kit, the mucosal samples were diluted to 2 mg protein per milliliter. After adding the samples, the reaction was incubated for 1 h at room temperature. The anti-autotaxin antibody and the secondary detector were then added followed by incubation for an additional hour. After stopping the reaction and color generation, the absorbance was assayed at 450 nm. Standard samples with different concentrations of autotaxin were assayed simultaneously. The levels of autotaxin in each sample were determined with reference of the standard curve generated.

Statistical analysis

Statistical significance for multiple comparisons was determined by one-way ANOVA followed by Newman-Keuls analysis using Prism 5.0 (GraphPad Software). All data are presented as the mean ± SEM from at least three repeated experiments. $P < 0.05$ was defined as statistically significant.

RESULTS

Changes of body weight and DAI in KO and WT mice

As shown in **Fig. 1A**, the body weights of both WT and the Alk-SMase KO mice were stable for the first 3 days and started decreasing on day 4. The reduction was greater in KO than in WT mice. At the end of the experiment, the body weight had decreased by 30% in KO mice and by 23% in WT mice. Although WT and KO mice started showing blood stain on stool or anus on day 5, bloody diarrhea rapidly occurred and became more serious in KO than in WT mice. At day 8, most stools in the WT group were still shaped, while those in KO group showed serious bloody diarrhea. The KO mice were also more sluggish than the WT mice. Thus the DAI in KO mice was significantly higher than in WT mice from day 6 to day 8 (Fig. 1B).

TABLE 2. Macroscopic change score of the colitis

Score	Edema	Bleeding	Ulceration
0	None	None	None
1	Mild	Mild	Mild
2	Moderate	Moderate	Moderate
3	Severe	Severe	Severe

Macroscopic changes in KO and WT mice

Macroscopic signs of inflammation in the colon were found in both groups, but the severity was greater in KO than in WT mice. KO mice exhibited broader mucosal bleeding, more extensive tissue edema, and more severe ulceration, as shown by a pair of representative samples in **Fig. 2A**. Compared with WT mice, the length of the colon in KO mice was significantly shortened (Fig. 2B). The more pronounced tissue edema, bleeding, and visible ulcerations in KO mice gave a significantly higher macroscopic index (Fig. 2C). The wet weights of thymus and liver were significantly reduced and that of spleen slightly increased ($P = 0.134$) in KO mice compared with WT mice (Fig. 2D).

Histopathological changes of the colon in KO and WT mice

Histopathological characterization revealed more marked damage of the crypts in KO mice. As shown in **Fig. 3A**, the height of the mucosa in KO mice was shortened, the surface was more irregular, and the destruction of the crypt architecture was more obvious (arrowed) compared with WT mice. Figure 3B shows detailed pathological changes with higher magnifications. A larger number of inflammatory cells and broader infiltrations, even to serosa, were observed in KO mice (Fig. 3Ba, d); whereas in WT mice, the infiltration was largely spread to muscularis (Fig. 3Bd). Glandular hyperplasia in KO mice was more severe (Fig. 3Bb) than in WT mice (Fig. 3Bc). Diffusion of inflammatory cells to blood vessels was observed in both groups [KO (Fig. 3Bc) and WT (Fig. 3Ba)], with that in KO mice more extensive. Figure 3Bb (WT) shows the tendency of inflammatory cells to form follicles. In addition, goblet cell reduction, nucleus distortion, and colonic erosion were more obvious in KO (Fig. 3Bb) than in WT mice (Fig. 3Bc). These changes led to higher microscopic inflammatory scores in KO than in WT mice (Fig. 3C).

Changes of PAF and LPA in KO and WT mice

In order to find potential mechanisms for the more severe colitis in Alk-SMase KO mice, we examined two inflammatory

TABLE 3. Histology score of the colitis

Changes	Score	Degree
Damage of epithelium	0	Morphologically normal
	1	Zonal destruction of the epithelial surface
	2	Diffuse epithelial destruction and/or mucosal ulcerations involving submucosa
	3	Severe epithelial destruction
Inflammatory cell infiltration	0	Absence of infiltrate or fewer than five cells
	1	Mild infiltration to the lamina propria
	2	Moderate infiltration to the muscularis mucosae
	3	High infiltration to the muscularis mucosae
	4	Severe infiltration involving the submucosa
Goblet cell depletion	0	No depletion
	1	Presence of nonorganized goblet cells
	2	Presence of one to three areas without goblet cells
	3	More than three areas without goblet cells
	4	Complete depletion of goblet cells
Crypt damage	0	None
	1	One-third of crypt damaged
	2	Two-thirds of crypt damaged
	3	Crypts lost, surface epithelium intact
	4	Crypts lost, surface epithelium lost
Percent involvement	0	0
	1	1–25%
	2	26–50%
	3	51–75%
	4	76–100%

lysophospholipids, PAF and LPA, which are closely related to the substrates of Alk-SMase (3). As shown in **Fig. 4**, before DSS treatment (day 0), the levels of PAF and LPA in WT and KO mice were all low. However, after 2 days of DSS treatment, PAF in the KO mice was significantly higher than that in the WT group. The increase of PAF in WT mice occurred later than in KO mice. The increase reached maximal levels on day 4 in both groups and declined on day 8. The levels of PAF on day 8, although low, were still significantly higher ($P < 0.05$) in KO mice than in WT mice. The LPA levels increased with time in both WT and KO mice, and the levels in KO mice were about 60% ($P < 0.05$) higher than those in WT mice on day 4 and 36% ($P < 0.05$) higher on day 8. Because LPA is mainly produced by autotaxin, we further examined the expression of autotaxin.

Changes of autotaxin expression in both small intestine and colon in KO and WT mice

We first studied the expression of autotaxin by IHC methods. The results from small intestine are shown in **Fig. 5A**, and those from colon in Fig. 5B. In the small intestine, before DSS treatment (day 0), there was a dispersed weak expression (brown stains), which was identified in the lamina propria of the villi and was most likely produced by the immune cells (arrowed) in both WT and KO mice. On day 2, while the positive IHC staining in WT mice was only slightly increased, that in KO mice was significantly intensified. Expression was also found in the endothelial cells of blood vessels or high epithelial venule-like structures (arrowed). On day 4, higher expression was found in both groups and the positive staining was mainly displayed along the middle of the lamina propria in the conduit system (arrowed). As in colon (Fig. 5B), there was no positive staining identified before DSS treatment (day 0) in either WT or KO mice, but it became clearly visible on day 2, with the expression more intensive in KO than in WT mice. The expression was also found in the lamina propria region of the crypt in some types of immune cells (arrowed). The expression of autotaxin on day 4 in the colon was sharply increased for both WT and KO mice, the increase in KO mice being more pronounced. Expression in the endothelial cells of blood vessels in the colon was also identified in both WT and KO mice (Fig. 5C). However, expression of autotaxin was not found on the surface of the mucosa in either the small intestine or the colon. Due to the severe damage of the colonic mucosa, the IHC results on day 8 could not be interpreted (not shown). In addition, Fig. 5A and B also show that on day 0, no inflammation signs were identified for either WT or KO mice, indicating that the lack of Alk-SMase alone did not induce colitis.

To compare the intensity of autotaxin expression between WT and KO mice, Western blot for autotaxin on day 4 was performed and the densities of the bands were determined. As shown in the right panels of **Fig. 6**, the autotaxin bands in KO and WT mice treated with DSS were clearly demonstrated in both small intestine and colon, with the expression more obvious in KO than in WT mice. The densities of the bands are shown in the left panels of Fig. 6. The autotaxin expression was approximately 98% higher in the small intestine and 77% higher in the colon in KO mice than in WT mice.

To confirm the semi-quantitative results from Western blot, autotaxin was further determined by sandwich ELISA 4 days after DSS treatment of the mice (**Fig. 7**). In support of the results from Western blot, the levels of autotaxin

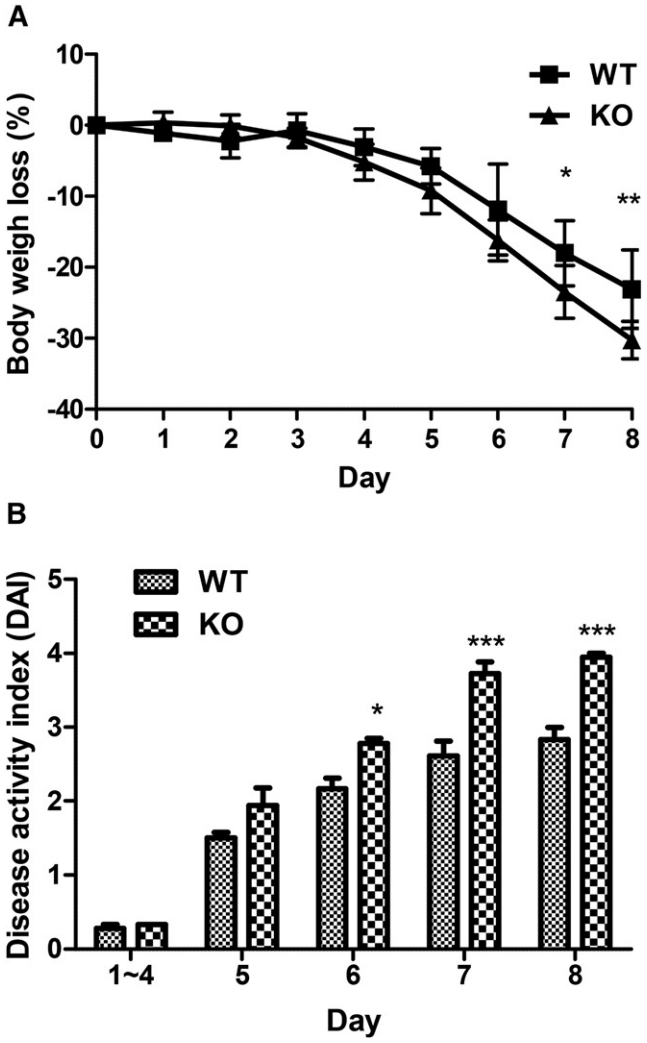

Fig. 1. Changes of the body weight and DAI. The animals were treated with DSS for 8 days. The body weight was measured, stool consistency and disease signs recorded, and DAI calculated according to Table 1. The changes of body weight in percentage of the original values on day 0 are shown in panel A and DAI in panel B. N = 6 for each group. $*P < 0.05$, $**P < 0.01$, $***P < 0.005$ compared with WT.

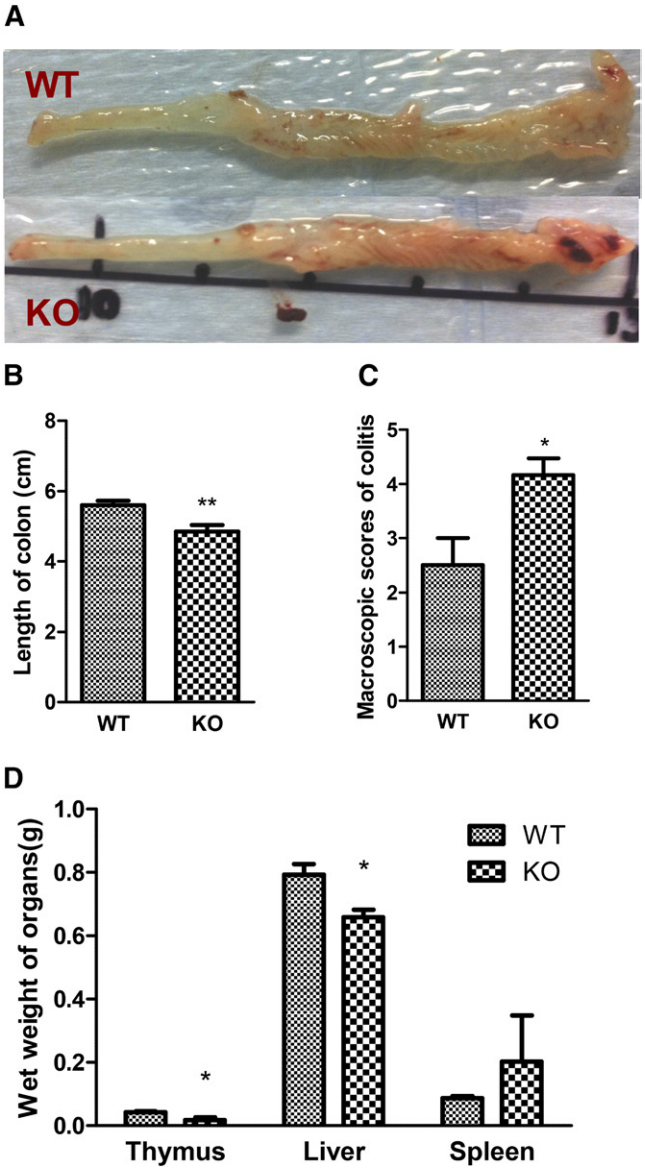

Fig. 2. Macroscopic changes between WT and KO mice. The mice were treated with DSS for 8 days. The colon was removed and opened longitudinally. A: A representative pair of colons from WT and KO mice showing more severe mucosal edema, bleeding, and ulceration in KO compared to WT mice. The length of colon is shown in panel B. The macroscopic injury scores, according to Table 2, are shown in panel C. The differences of wet weights of thymus, liver, and spleen are shown in panel D. N = 6 for each group. $*P < 0.05$ and $**P < 0.01$ compared with WT.

were six to seven times higher in KO than in WT mice for both small intestine and colon.

Changes of IL6, IL10, and TNFα in KO and WT mice

The changes of the cytokines, IL6, IL10, and TNFα, after DSS treatment in KO and WT mice are shown in **Fig. 8**. These cytokines were low on days 0 and 2 when inflammation signs did not display. However, at this time point, notably lower IL10 levels were demonstrated in KO mice than in WT mice. DSS treatment induced increases of both IL10 and IL6 on day 4, followed by a significant reduction on day 8 in both WT and KO mice, with the decrease in KO mice more obvious than in WT mice. TNFα showed a time-dependent increase in both WT and KO mice. No difference was found from day 0 to day 4, but the levels on day 8 in KO mice were significantly lower than in WT mice.

DISCUSSION

In the present study, we examined DSS-induced colitis in Alk-SMase KO mice and WT mice. We found that the deficiency of Alk-SMase significantly enhanced the inflammation, as shown by the greater loss of body, thymus, and liver weights, by more severe bloody diarrhea and mucosal injury, and by microscopic findings of crypt distortion and more intensive inflammatory cell infiltration. Earlier studies suggested that Alk-SMase might indeed have anti-inflammatory functions in the gut. Patients with chronic ulcerative colitis had lowered Alk-SMase

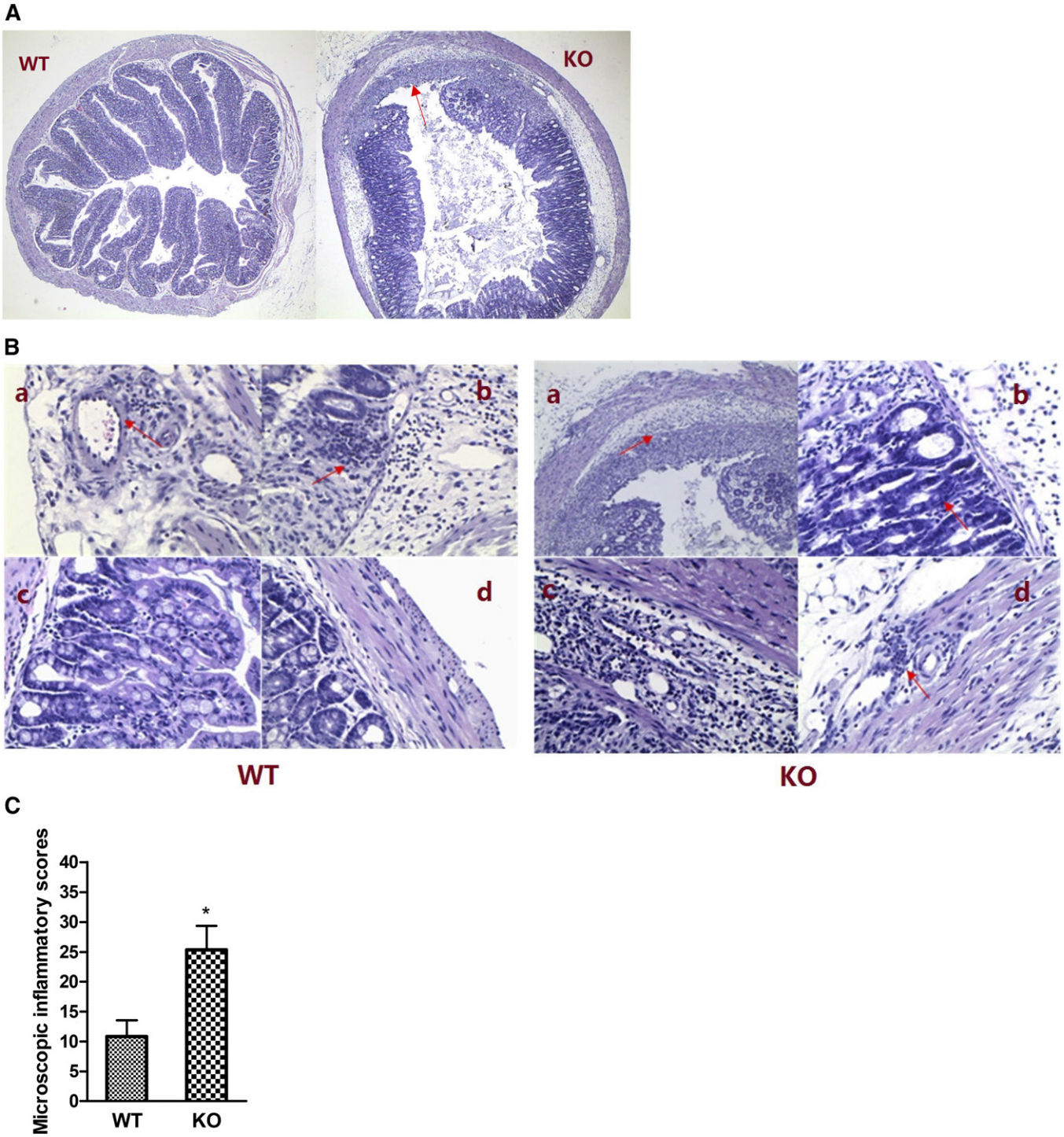

Fig. 3. Histopathological characterization of colons in Alk-SMase KO and WT mice. After treating the mice with DSS for 8 days, the colon was removed and observed histopathologically. A: Representative micrographs (×40) showing more severe epithelial destruction and infiltration in KO than in WT mice (arrowed). B: Details of the pathological changes. In the B panel for WT, inflammatory cells infiltrate the dilated and congested blood vessel (a); the large number of inflammatory cells and the tendency to form lymph follicles (b); less damaged epithelial cells and mild glandular atypical hyperplasia (c); and less inflammatory cell infiltration to the muscularis (d). In the B panel for KO, severe mucosal destruction, crypt damage, and intensive inflammatory cell infiltration to submucosa, muscularis, and serosa (a); severe glandular atypical hyperplasia, goblet cell depletion, and nucleus distortion (b); intensive hemangiectasis and infiltration of inflammatory cells to blood vessel and submucosa (c); and intensive inflammatory cells infiltrated to serosa (d). C: The histopathological scores according to Table 3. N = 6 for each group. $*P < 0.05$ compared with WT.

activity (12), and recombinant human Alk-SMase given rectally alleviated DSS-induced acute colitis in rats (22). Furthermore, it was recently reported that upregulation of the ENPP7 gene is a feature of the immunosuppressive response to chronic infection with enterohemorrhagic *Escherichia coli* in calves (24). The present study provides

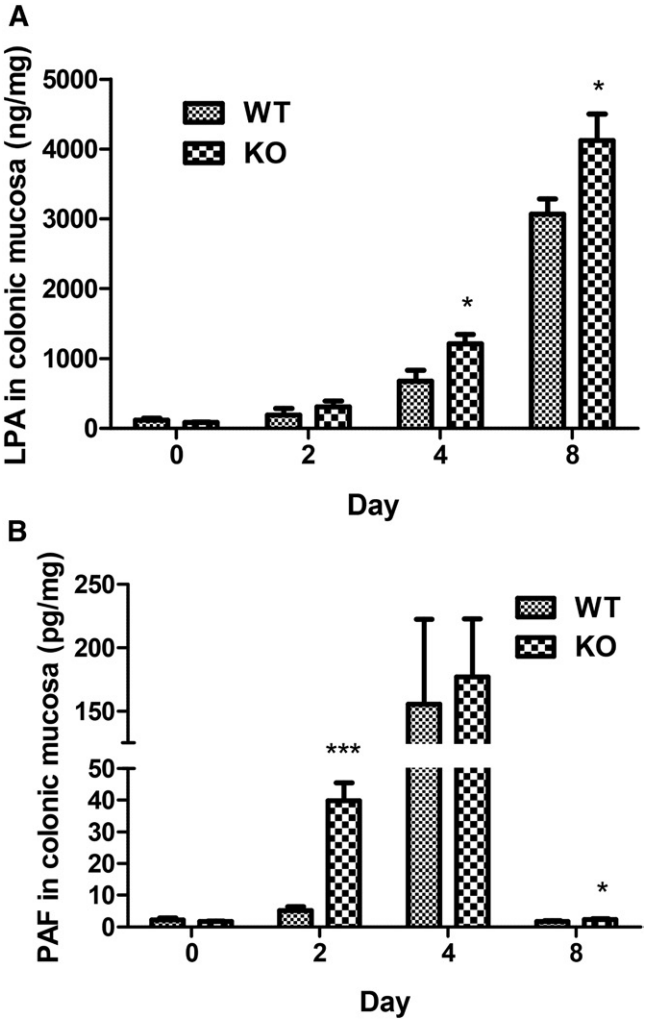

Fig. 4. Changes of PAF and LPA in colonic mucosa. The animals were treated with DSS and euthanized on days 0, 2, 4, and 8, respectively. PAF and LPA in colonic mucosa were assayed by ELISA and the results are shown in panels A and B, respectively. N = 4 for day 0, 2, and 4 observations; N = 6 for day 8 observation for both WT and KO mice. $*P < 0.05$, $***P < 0.005$ compared with the WT.

strong direct evidence that Alk-SMase not only plays crucial roles in digestion of dietary SM (2) and cholesterol absorption (25), but also protects intestinal mucosa against inflammation. Thereby the results also deepen our understanding of the finding that colitis-associated carcinogenesis was enhanced in Alk-SMase KO mice (14).

In relation to the potential mechanisms of the enhancement of DSS colitis in the KO mice, a major finding was the greater increase of LPA levels and the upregulation of autotaxin in the colonic mucosa. The autotaxin-LPA axis is an important signaling pathway in inflammation and cancer (26). Expression of autotaxin has been identified in several organs, including brain, placenta, ovary, respiratory tract, and intestinal tract (27, 28). Extracellular LPA is mainly generated by autotaxin and is an important lipid messenger, which promotes inflammatory responses via various G protein-coupled receptors, resulting in lymphocyte migration, MAPK activation, and Cox2 activation, to list a few (18). We found that, before DSS treatment, autotaxin was expressed at low levels in small intestine and hardly detectable in colon in both WT and KO mice, which is in agreement with reports by others (27, 28). Under physiological conditions, Alk-SMase is thus unlikely to have any profound influence on autotaxin expression. However, induction of inflammation by DSS triggered autotaxin expression in the colon and enhanced its expression in the small intestine, as also reported by others (29). Our novel finding that the degree of autotaxin expression was significantly higher in Alk-SMase KO mice than in WT mice indicates that Alk-SMase suppresses this upregulation of autotaxin by DSS. Also, the levels of LPA, i.e., the hydrolytic product of autotaxin activity against lyso-PC, increased more in the KO mice than in the WT mice. Because Alk-SMase has phospholipase C activity against lyso-PC, more lyso-PC generated by pancreatic and mucosal phospholipases (30, 31) may accumulate in the KO mice and increase substrate availability, which may thereby contribute to increased LPA formation by the phospholipase D activity of autotaxin. Whether this is so and whether lyso-PC may induce autotaxin expression are interesting questions for further study. Considering the strong evidence for a role of autotaxin and LPA in both human inflammatory bowel disease (IBD) and DSS colitis (29), we postulate that LPA signaling is an important factor behind the more severe inflammation in KO mice found in this study.

Interestingly, upregulation of autotaxin was also found in the small intestine in both WT and KO mice after DSS treatment. The changes were more obvious in KO mice than in WT mice. Yet, there were no signs of inflammation. The finding indicates a role of alk-SMase in also regulating autotaxin expression in the small intestine. The reason there are no signs of inflammation in the small intestine is likely due to the fact that DSS in the dose used selectively induces inflammation in the colon but not in the small intestine (32). We recently also found that inflammation-associated tumorigenesis induced by azoxymethane/DSS occurred only in the colon but not in the small intestine in alk-SMase KO mice (14), although signs of hypertrophy were identified in the small intestine.

The mechanisms of the enhanced autotaxin expression in Alk-SMase KO mice may be multiple. One interesting finding was the marked increase of PAF that occurred on day 2 in the KO mice, which was earlier than that in WT mice. At this time point, increased expression of autotaxin was clearly demonstrated in the small intestine and colon of the KO mice (Fig. 5B). PAF is synthesized in many types of cells, including endothelial cells and epithelial cells, in response to inflammatory factors (33). The colon actively synthesizes PAF, and both PAF receptors and PAF acetyl hydrolase have been identified in colonic mucosa (34, 35). High PAF levels have been reported in patients with IBD and in DSS-treated animals (34, 36). The newly synthesized PAF stimulates inflammation, which may in turn trigger higher expression of autotaxin in the inflamed mucosa. Based on our previous finding that PAF is one of the

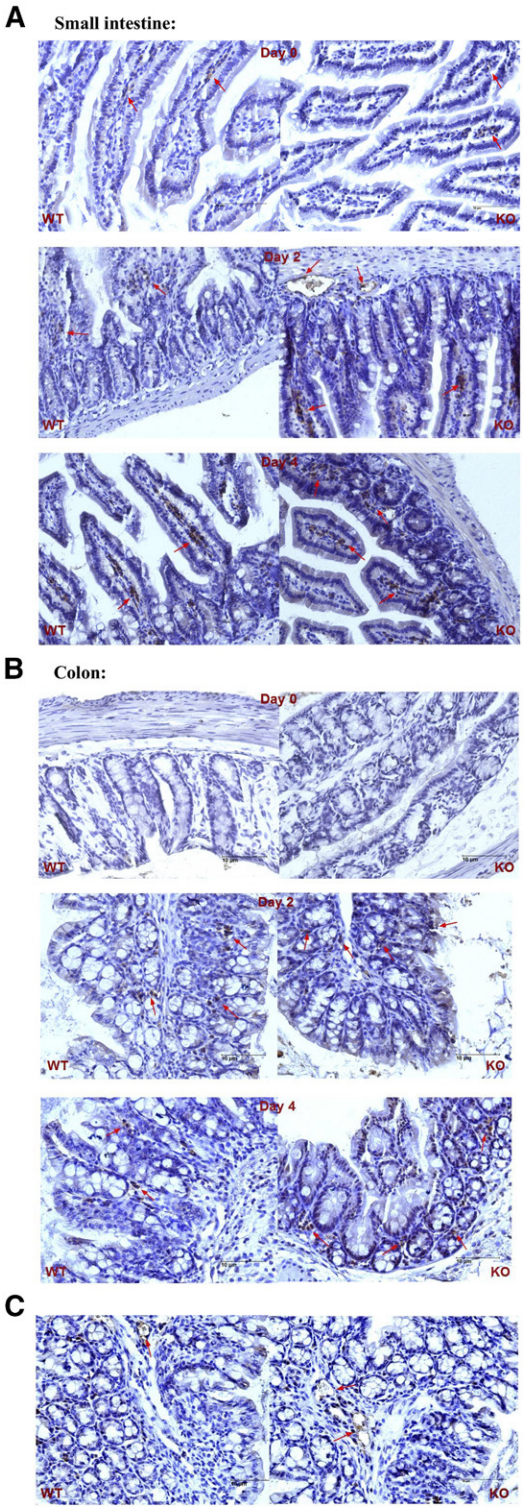

Fig. 5. Autotaxin expression in both small intestine and colon. The animals were treated with DSS for 2 and 4 days and the expression of autotaxin in small intestine and colon treatment was studied by IHC. A: The autotaxin expression in the small intestine. As indicated by the arrows, the expression was weak on day 0 and increased thereafter. The increase is more obvious in KO than in WT mice. The expression is mainly in the lamina propria of villi and vessels (arrowed). B: The autotaxin expression in the colon. Essentially no positive stain was identified before DSS treatment (day 0) in both WT and KO groups, but was obviously visible on day 2 and day 4, with that in KO mice being more intensive than in the WT group. The expression was also by endothelial and immune cells (arrowed) in the lamina propria region of the crypt. C: The expression of autotaxin in the endothelium of blood vessels on day 4 in WT and KO mice.

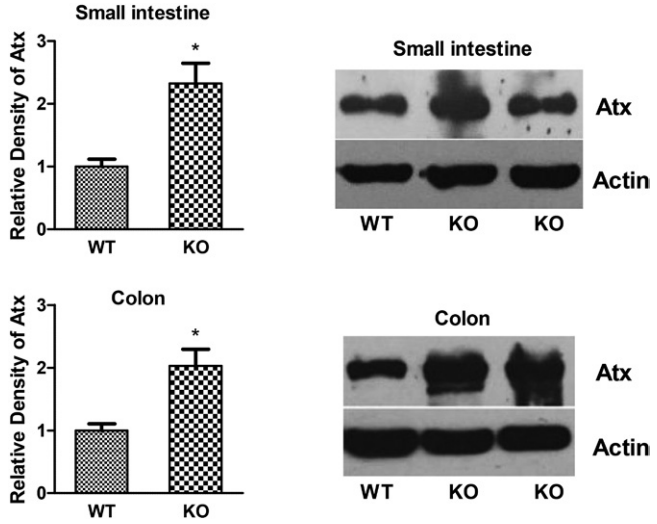

Fig. 6. Western blot for autotaxin (Atx) in the small intestine and colon. The animals were treated with DSS for 4 days. Western blot for autotaxin was performed in the homogenates of both colonic and small intestinal mucosa. The right panels show the representative results of one experiment. The densities of the bands from all mice were determined related to that in the WT group. N = 3 for both WT and KO mice. $^{*}P < 0.05$ compared with WT mice.

substrates of Alk-SMase, lack of Alk-SMase can cause an early accumulation of PAF or accelerate the production of PAF in response to inflammatory factors, as previously speculated (3, 5).

We also examined changes of two central pro-inflammatory cytokines, TNFα and IL6, and one important anti-inflammatory cytokine, IL10, which have been thought to play key roles in IBD. As we found a similar increase of TNFα in both WT and KO mice, we could thus not link increased TNFα to the more severe inflammation or the increased autotaxin levels in the KO mice, although TNFα was reported to stimulate autotaxin expression in some types of human hepatocellular carcinomas (37). We also could not link increased IL6 levels to the more severe inflammation and autotaxin expression in KO mice, although IL6 was found to stimulate autotaxin expression in adipocytes (38). In addition, lower levels of IL10 in Alk-SMase KO mice were observed early in the time course. Because IL10 is considered to be an anti-inflammatory cytokine, the decreased IL10 found in this study may increase sensitivity of the KO mice to DSS and thus facilitate autotaxin expression. A limitation of the present study is that we did not study the changes of other cytokines, particularly IL1α, IL1β, and IL4, which may also affect autotaxin expression (39, 40). Another limitation is that we don't have a clear interpretation of the decline of PAF,

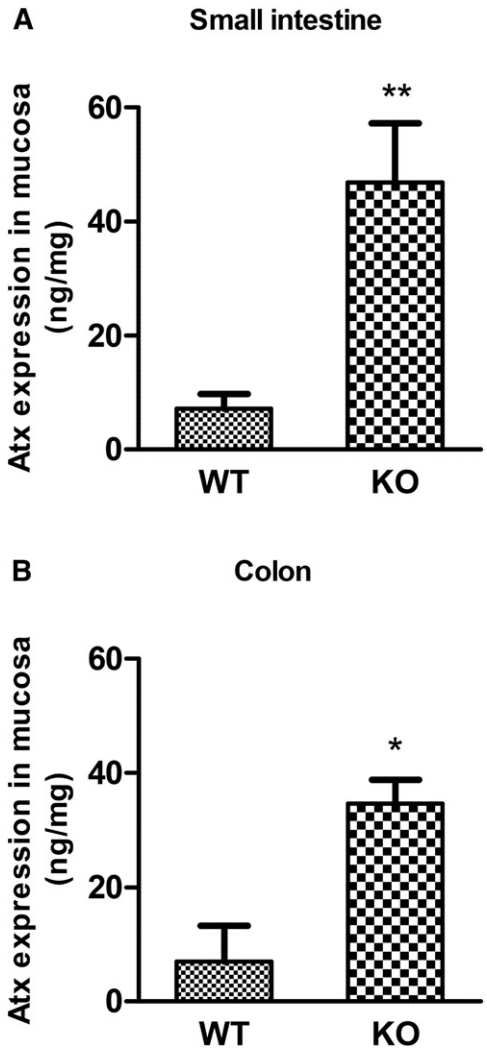

Fig. 7. ELISA for autotaxin (Atx) in the small intestine (A) and colon (B). The WT and KO mice were treated with DSS for 4 days. The autotaxin levels were assayed in the homogenates of both colonic and small intestinal mucosa. N = 4 for both WT and KO mice. $*P < 0.05$, $**P < 0.01$ compared with the WT mice.

IL6, and IL10 in the colonic mucosa at the late stage (day 8) when the inflammation was most severe. These reductions might be related to the severe destruction of the mucosal architecture or to counter-regulatory mechanisms, as reported and discussed previously by others (41). More extensive studies on changes of both pro-inflammatory and anti-inflammatory cytokines and their relation to autotaxin expression and LPA formation, sphingolipid metabolism, and the time course for colitis development are needed. Finally, the changes of thymus, liver, and spleen weights shown in this study were in agreement with previous report (42), and also support more severe inflammation in KO than in WT mice. The relation between these changes, cytokine levels, and immune cell functions remains elusive.

Altogether, we found that deficiency of Alk-SMase enhances colitis induced by DSS, possibly via the autotaxin-LPA pathway and an early rise in PAF. This study, thus, for the first time, identifies an interesting cross communication between Alk-SMase (NPP7) and autotaxin (NPP2), and PAF signaling, which may have important implications in inflammatory diseases and carcinogenesis.

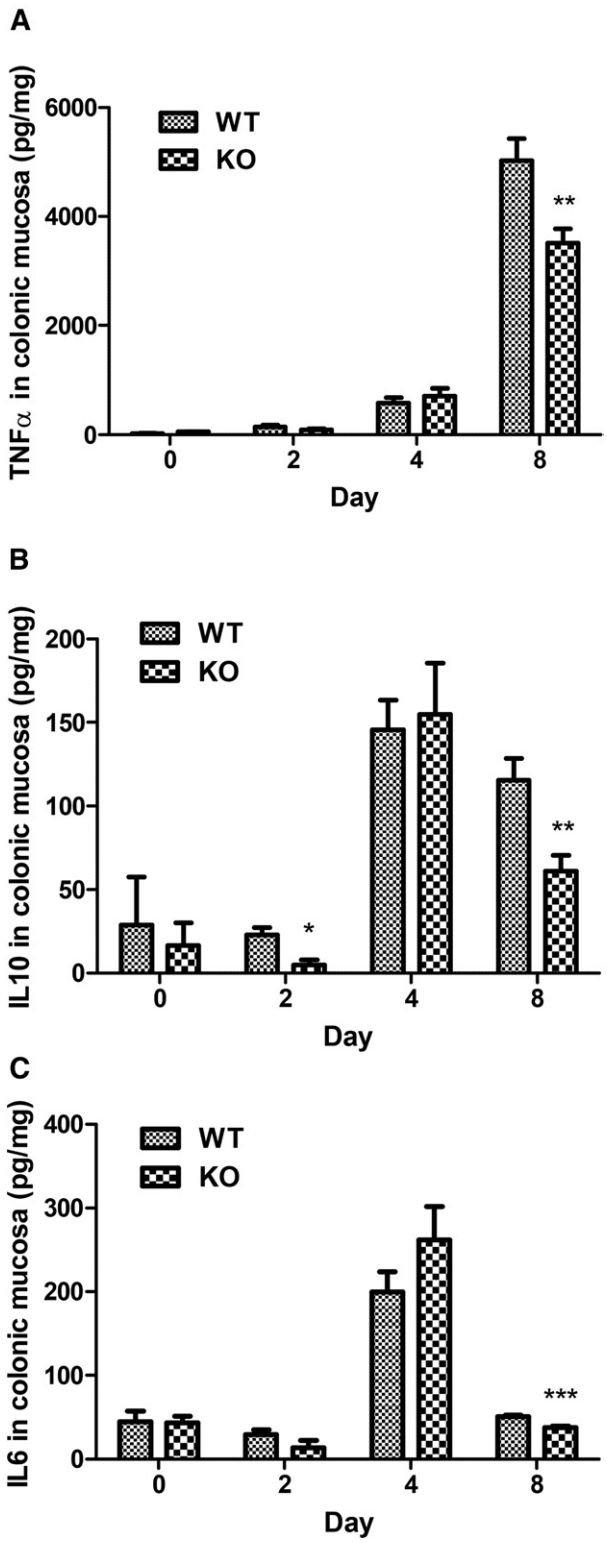

Fig. 8. Changes of TNFα (A), IL10 (B), and IL6 (C). The animals were treated with DSS and euthanized on days 0, 2, 4, and 8, respectively. The homogenates of colonic mucosa were prepared and the levels of TNFα, IL10, and IL6 were assayed with ELISA. N = 4 for day 0, 2, and 4 experiments; N = 6 for day 8 experiments for both WT and KO mice. $*P < 0.05$, $**P < 0.01$, $***P < 0.005$ compared with WT mice at each time point.

REFERENCES

1. Nilsson, Å. 1969. The presence of sphingomyelin- and ceramide-cleaving enzymes in the small intestinal tract. *Biochim. Biophys. Acta.* **176:** 339–347.
2. Zhang, Y., Y. Cheng, G. H. Hansen, L. L. Niels-Christiansen, F. Koentgen, L. Ohlsson, A. Nilsson, and R. D. Duan. 2011. Crucial role of alkaline sphingomyelinase in sphingomyelin digestion: a study on enzyme knockout mice. *J. Lipid Res.* **52:** 771–781.
3. Duan, R. D. 2006. Alkaline sphingomyelinase: an old enzyme with novel implications. *Biochim. Biophys. Acta.* **1761:** 281–291.
4. Duan, R. D., T. Bergman, N. Xu, J. Wu, Y. Cheng, J. Duan, S. Nelander, C. Palmberg, and A. Nilsson. 2003. Identification of human intestinal alkaline sphingomyelinase as a novel ecto-enzyme related to the nucleotide phosphodiesterase family. *J. Biol. Chem.* **278:** 38528–38536.
5. Wu, J., A. Nilsson, B. A. Jonsson, H. Stenstad, W. Agace, Y. Cheng, and R. D. Duan. 2006. Intestinal alkaline sphingomyelinase hydrolyses and inactivates platelet-activating factor by a phospholipase C activity. *Biochem. J.* **394:** 299–308.
6. Hannun, Y. A., and L. M. Obeid. 2008. Principles of bioactive lipid signalling: lessons from sphingolipids. *Nat. Rev. Mol. Cell Biol.* **9:** 139–150.
7. Moolenaar, W. H. 2002. Lysophospholipids in the limelight: autotaxin takes center stage. *J. Cell Biol.* **158:** 197–199.
8. Tsoupras, A. B., C. Iatrou, C. Frangia, and C. A. Demopoulos. 2009. The implication of platelet activating factor in cancer growth and metastasis: potent beneficial role of PAF-inhibitors and antioxidants. *Infect. Disord. Drug Targets.* **9:** 390–399.
9. Dillehay, D. L., S. K. Webb, E. M. Schmelz, and A. H. Merrill, Jr. 1994. Dietary sphingomyelin inhibits 1,2-dimethylhydrazine-induced colon cancer in CF1 mice. *J. Nutr.* **124:** 615–620.
10. Hertervig, E., A. Nilsson, J. Bjork, R. Hultkrantz, and R. D. Duan. 1999. Familial adenomatous polyposis is associated with a marked decrease in alkaline sphingomyelinase activity: a key factor to the unrestrained cell proliferation? *Br. J. Cancer.* **81:** 232–236.
11. Hertervig, E., A. Nilsson, L. Nyberg, and R. D. Duan. 1997. Alkaline sphingomyelinase activity is decreased in human colorectal carcinoma. *Cancer.* **79:** 448–453.
12. Sjöqvist, U., E. Hertervig, A. Nilsson, R. D. Duan, A. Ost, B. Tribukait, and R. Lofberg. 2002. Chronic colitis is associated with a reduction of mucosal alkaline sphingomyelinase activity. *Inflamm. Bowel Dis.* **8:** 258–263.
13. Zhang, P., B. Li, S. Gao, and R. D. Duan. 2008. Dietary sphingomyelin inhibits colonic tumorigenesis with an up-regulation of alkaline sphingomyelinase expression in ICR mice. *Anticancer Res.* **28:** 3631–3635.
14. Chen, Y., P. Zhang, S. C. Xu, L. Yang, U. Voss, E. Ekblad, Y. Wu, Y. Min, E. Hertervig, A. Nilsson, et al. 2015. Enhanced colonic tumorigenesis in alkaline sphingomyelinase (NPP7) knockout mice. *Mol. Cancer Ther.* **14:** 259–267.
15. Yost, C. C., A. S. Weyrich, and G. A. Zimmerman. 2010. The platelet activating factor (PAF) signaling cascade in systemic inflammatory responses. *Biochimie.* **92:** 692–697.
16. Wardle, T. D., L. Hall, and L. A. Turnberg. 1996. Platelet activating factor: release from colonic mucosa in patients with ulcerative colitis and its effect on colonic secretion. *Gut.* **38:** 355–361.
17. Yang, Y., E. M. Nemoto, S. A. Harvey, V. M. Subbotin, and C. R. Gandhi. 2004. Increased hepatic platelet activating factor (PAF) and PAF receptors in carbon tetrachloride induced liver cirrhosis. *Gut.* **53:** 877–883.
18. Knowlden, S., and S. N. Georas. 2014. The autotaxin-LPA axis emerges as a novel regulator of lymphocyte homing and inflammation. *J. Immunol.* **192:** 851–857.
19. Stracke, M. L., H. C. Krutzsch, E. J. Unsworth, A. Arestad, V. Cioce, E. Schiffmann, and L. A. Liotta. 1992. Identification, purification, and partial sequence analysis of autotaxin, a novel motility-stimulating protein. *J. Biol. Chem.* **267:** 2524–2529.
20. Tokumura, A., E. Majima, Y. Kariya, K. Tominaga, K. Kogure, K. Yasuda, and K. Fukuzawa. 2002. Identification of human plasma lysophospholipase D, a lysophosphatidic acid-producing enzyme, as autotaxin, a multifunctional phosphodiesterase. *J. Biol. Chem.* **277:** 39436–39442.
21. Stefan, C., S. Jansen, and M. Bollen. 2005. NPP-type ectophosphodiesterases: unity in diversity. *Trends Biochem. Sci.* **30:** 542–550.
22. Andersson,D.,K.Kotarsky,J.Wu,W.Agace,andR.D.Duan.2009.Expression of alkaline sphingomyelinase in yeast cells and anti-inflammatory effects of the expressed enzyme in a rat colitis model. *Dig. Dis. Sci.* **54:** 1440–1448.
23. Maines, L. W., L. R. Fitzpatrick, K. J. French, Y. Zhuang, Z. Xia, S. N. Keller, J. J. Upson, and C. D. Smith. 2008. Suppression of ulcerative colitis in mice by orally available inhibitors of sphingosine kinase. *Dig. Dis. Sci.* **53:** 997–1012.
24. Kieckens, E., J. Rybarczyk, R. W. Li, D. Vanrompay, and E. Cox. 2016. Potential immunosuppressive effects of Escherichia coli O157:H7 experimental infection on the bovine host. *BMC Genomics.* **17:** 1049.
25. Zhang, P., Y. Chen, Y. Cheng, E. Hertervig, L. Ohlsson, A. Nilsson, and R. D. Duan. 2014. Alkaline sphingomyelinase (NPP7) promotes cholesterol absorption by affecting sphingomyelin levels in the gut: A study with NPP7 knockout mice. *Am. J. Physiol. Gastrointest. Liver Physiol.* **306:** G903–G908.
26. van Meeteren, L. A., and W. H. Moolenaar. 2007. Regulation and biological activities of the autotaxin-LPA axis. *Prog. Lipid Res.* **46:** 145–160.
27. Giganti, A., M. Rodriguez, B. Fould, N. Moulharat, F. Coge, P. Chomarat, J. P. Galizzi, P. Valet, J. S. Saulnier-Blache, J. A. Boutin, et al. 2008. Murine and human autotaxin alpha, beta, and gamma isoforms: gene organization, tissue distribution, and biochemical characterization. *J. Biol. Chem.* **283:** 7776–7789.
28. Lee, H. Y., J. Murata, T. Clair, M. H. Polymeropoulos, R. Torres, R. E. Manrow, L. A. Liotta, and M. L. Stracke. 1996. Cloning, chromosomal localization, and tissue expression of autotaxin from human teratocarcinoma cells. *Biochem. Biophys. Res. Commun.* **218:** 714–719.
29. Hozumi, H., R. Hokari, C. Kurihara, K. Narimatsu, H. Sato, S. Sato, T. Ueda, M. Higashiyama, Y. Okada, C. Watanabe, et al. 2013. Involvement of autotaxin/lysophospholipase D expression in intestinal vessels in aggravation of intestinal damage through lymphocyte migration. *Lab. Invest.* **93:** 508–519.
30. Hui, D. Y. 2016. Intestinal phospholipid and lysophospholipid metabolism in cardiometabolic disease. *Curr. Opin. Lipidol.* **27:** 507–512.
31. Nilsson, A. 1968. Intestinal absorption of lecithin and lysolecithin by lymph fistula rats. *Biochim. Biophys. Acta.* **152:** 379–390.
32. Okayasu, I., S. Hatakeyama, M. Yamada, T. Ohkusa, Y. Inagaki, and R. Nakaya. 1990. A novel method in the induction of reliable experimental acute and chronic ulcerative colitis in mice. *Gastroenterology.* **98:** 694–702.
33. Chao, W., and M. S. Olson. 1993. Platelet-activating factor: receptors and signal transduction. *Biochem. J.* **292:** 617–629.
34. Merendino, N., M. B. Dwinell, N. Varki, L. Eckmann, and M. F. Kagnoff. 1999. Human intestinal epithelial cells express receptors for platelet-activating factor. *Am. J. Physiol.* **277:** G810–G818.
35. Riehl, T. E., and W. F. Stenson. 1995. Platelet-activating factor acetylhydrolases in Caco-2 cells and epithelium of normal and ulcerative colitis patients. *Gastroenterology.* **109:** 1826–1834.
36. Ferraris, L., F. Karmeli, R. Eliakim, J. Klein, C. Fiocchi, and D. Rachmilewitz. 1993. Intestinal epithelial cells contribute to the enhanced generation of platelet activating factor in ulcerative colitis. *Gut.* **34:** 665–668.
37. Wu, J. M., Y. Xu, N. J. Skill, H. Sheng, Z. Zhao, M. Yu, R. Saxena, and M. A. Maluccio. 2010. Autotaxin expression and its connection with the TNF-alpha-NF-kappaB axis in human hepatocellular carcinoma. *Mol. Cancer.* **9:** 71.
38. Sun, S., R. Wang, J. Song, M. Guan, N. Li, X. Zhang, Z. Zhao, and J. Zhang. 2017. Blocking gp130 signaling suppresses autotaxin expression in adipocytes and improves insulin sensitivity in diet-induced obesity. *J. Lipid Res.* **58:** 2102–2113.
39. Benesch, M. G., Y. Y. Zhao, J. M. Curtis, T. P. McMullen, and D. N. Brindley. 2015. Regulation of autotaxin expression and secretion by lysophosphatidate and sphingosine 1-phosphate. *J. Lipid Res.* **56:** 1134–1144.
40. Kehlen, A., R. Lauterbach, A. N. Santos, K. Thiele, U. Kabisch, E. Weber, D. Riemann, and J. Langner. 2001. IL-1 beta- and IL-4-induced down-regulation of autotaxin mRNA and PC-1 in fibroblast-like synoviocytes of patients with rheumatoid arthritis (RA). *Clin. Exp. Immunol.* **123:** 147–154.
41. Egger, B., M. Bajaj-Elliott, T. T. MacDonald, R. Inglin, V. E. Eysselein, and M. W. Buchler. 2000. Characterisation of acute murine dextran sodium sulphate colitis: cytokine profile and dose dependency. *Digestion.* **62:** 240–248.
42. Sasaki, S., Y. Ishida, N. Nishio, S. Ito, and K. Isobe. 2008. Thymic involution correlates with severe ulcerative colitis induced by oral administration of dextran sulphate sodium in C57BL/6 mice but not in BALB/c mice. *Inflammation.* **31:** 319–328.